Second-order advantage with excitation-emission photoinduced fluorimetry for the determination of the antiepileptic carbamazepine in environmental waters

Valeria A. Lozano, Graciela M. Escandar*

Instituto de Química Rosario (CONICET-UNR), Facultad de Ciencias Bioquímicas y Farmacéuticas, Universidad Nacional de Rosario, Suipacha 531 (2000) Rosario, Argentina. E-mail: escandar@iquir-conicet.gov.ar

Abstract

A photochemically-induced fluorescence system combined with second-order chemometric analysis for the determination of the anticonvulsant carbamazepine (CBZ) is presented. CBZ is a widely used drug for the treatment of epilepsy and is included in the group of emerging contaminant present in the aquatic environment. CBZ is not fluorescent in solution but can be converted into a fluorescent compound through a photochemical reaction in a strong acid medium. The determination is carried out by measuring excitation-emission photoinduced fluorescence matrices of the products formed upon ultraviolet light irradiation in a laboratory-constructed reactor constituted by two simple 4 W germicidal tubes. Working conditions related to both the reaction medium and the photoreactor geometry are optimized by an experimental design. The developed approach enabled the determination of CBZ at trace levels without the necessity of applying separation steps, and in the presence of uncalibrated interferences which also display photoinduced fluorescence and may be potentially present in the investigated samples. Different second-order algorithms were tested and successful resolution was achieved using multivariate curve resolution-alternating least-squares (MCR-ALS). The study is employed for the discussion of the scopes and yields of each of the applied second-order chemometric tools. The quality of the proposed method is probed through the determination of the studied emerging pollutant in both environmental and drinking water samples. After a pre-concentration step on a C18 membrane using 50.0 mL of real water samples, a prediction relative error of 2 % and limits of detection and quantification of 0.2 and 0.6 ng mL^{-1} were respectively obtained.

Keywords:

Photoinduced fluorescence

Multivariate calibration

Carbamazepine

1. Introduction

Carbamazepine (CBZ), 5H-dibenzo[*b*,*f*]azepine-5-carboxamide (Fig. 1) is an anticonvulsant drug widely used for the treatment of epilepsy and psychiatric diseases [1], and is included in the group of emerging contaminants [2]. This pharmaceutical pollutant is of particular concern because of its important toxicological and pharmacological effects in mammals, humans and the aquatic environment [3–6], in addition to the harmful consequences produced by its major photoproduct, acridine [7,8].

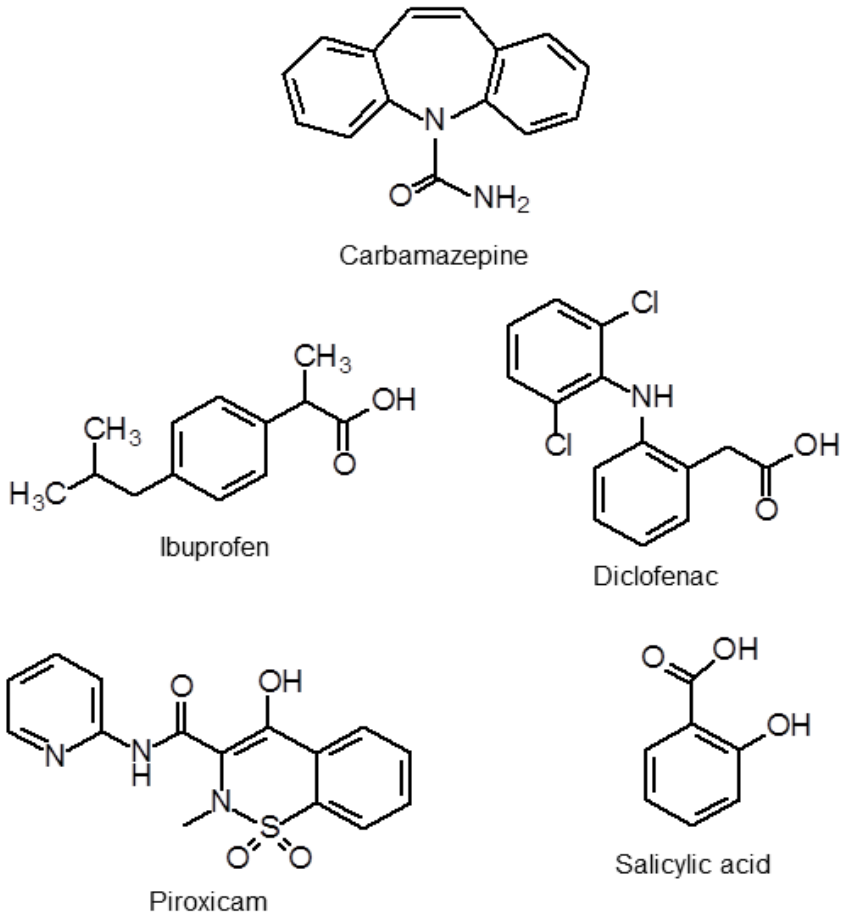

Fig. 1 Structure of carbamazepine and potential interferences.

Environmental studies have demonstrated that CBZ is one of the most frequently detected pharmaceutical in sewage-treatment plant effluents, river water and drinking water [9,10]. A

field study of occurrence and fate of CBZ and other five pharmaceuticals in surface waters of Switzerland concluded that CBZ reached concentrations of 0.4 and 0.95 ng mL^{-1} in river and wastewater treatment plant effluents, respectively [11]. An European Union (EU) monitoring study for organic compounds in rivers and streams across Europe indicated that CBZ is one of the most frequently detected compound (95%), with an average concentration of 0.25 ng mL^{-1} and maximum concentrations of about 11 ng mL^{-1} [12]. A recent study related to the occurrence of polar organic pollutants in EU ground waters included CBZ in the list of most frequently found pharmaceuticals (42.1 %), with a maximum concentration of 0.39 ng mL^{-1} [13].

CBZ seems to be persistent in the environment, therefore qualifying as a suitable marker for anthropogenic influences on the aquatic environment [14]. The determination of CBZ and atrazine was employed as a target analysis for tracers of organic contamination in drinking and surface waters, resulting in a useful tool to prioritize samples which should be further screened for suspect contaminants [15].

Very recently, during the analysis of selected pharmaceuticals in fish and surface waters directly affected by irrigation with reclaimed water, CBZ was consistently detected, with a significant bioaccumulation factor in mosquito fish [16].

Chromatographic methods are the most commonly applied ones for the determination of CBZ or its photodegradation products in different matrices [9–39], although spectrophotometric, mass spectrometric, electrochemical and capillary electrophoretic methods have also been proposed [40–47]. Since CBZ is not fluorescent in solution, fluorimetric methods for its determination have been developed in a nylon surface [48] or through the formation of fluorescent derivatives by oxidation with Ce(IV) [49,50], permanganate [51] and lead dioxide [52], or by photochemical reaction [53].

The determination of contaminants in complex samples brings the problem of the presence of interfering agents which must be removed, extending the analysis time and the experimental work. On the other hand, these separative steps frequently involve the use of organic solvents which are harmful to health and pollute the environment. In this regard, with the purpose of contributing with the protection of the environment and decreasing the health impact, there is a particular interest in developing methods for analytes of ecological concern complying with the principles of green analytical chemistry [54,55].

In this paper, we present a new and safe photochemically-induced fluorescence system for the determination of CBZ in environmental water samples without involving organic solvents. An acidic solution of CBZ is irradiated with two germicidal UV lamps, and the concentration of the formed photoproducts is then spectrofluorimetrically determined in the presence of pharmaceuticals (or their photoproducts) usually detected in the aquatic environment, coupling excitation-emission photoinduced fluorescence matrices (EEPIFMs) to multivariate calibration. Four chemometric algorithms which achieve the second order advantage, namely, parallel factor analysis (PARAFAC) [56] unfolded partial least-squares coupled to residual bilinearization (U-PLS/RBL) [57,58], multidimensional partial least-squares [59] coupled to residual bilinearization (N-PLS/RBL), and multivariate curve resolution-alternating least-squares (MCR-ALS) [60] were applied to process the EEPIFMs. Second-order advantage refers the capacity of certain second-order algorithms to predict concentrations of sample components in the presence of any number of unsuspected constituents [61,62]. Notable differences in the prediction capabilities of the employed algorithms were observed and discussed, and the feasibility of determining CBZ in natural water samples is demonstrated.

2. Experimental

2.1. Reagents and solutions

CBZ was obtained from Sigma (St. Louis, MO, USA). Methanol and hydrochloric acid were purchased from Merck (Darmstadt, Germany). Compounds tested as potential interferents were of analytical grade and were used as received. The stock solution of CBZ (530 μg mL^{-1}) was prepared in methanol. From this solution, more diluted aqueous working solutions were obtained. Ultrapure Milli-Q water was used throughout the work.

2.2. Instrumentation

Fluorescence spectra were measured using an Aminco Bowman (Rochester, NY, USA) Series 2 luminescence spectrometer equipped with a 150 W xenon lamp. These spectra were obtained using excitation and emission wavelengths of 308 and 410 nm, respectively, and both the excitation and emission slit widths were of 8 nm using 1.00 cm quartz cells. The photomultiplier tube (PMT) sensitivity was fixed at 700 V and the temperature of the cell compartment was kept constant at 20 ºC by circulating water from a thermostatted bath (Cole-Parmer, Illinois, USA).

2.3. Procedure

The photodegradation reaction was carried out in a very simple reactor constructed in our laboratory, constituted by two germicidal tubes of 4 W (Fig. 2). Both the geometry of the photoreactor and the experimental conditions to reach the best signal were optimized (see

below). EEPIFMs were measured from 280 to 320 nm (each 2 nm) and from 380 to 450 nm (each 1 nm), respectively, and were then subjected to second-order data analysis.

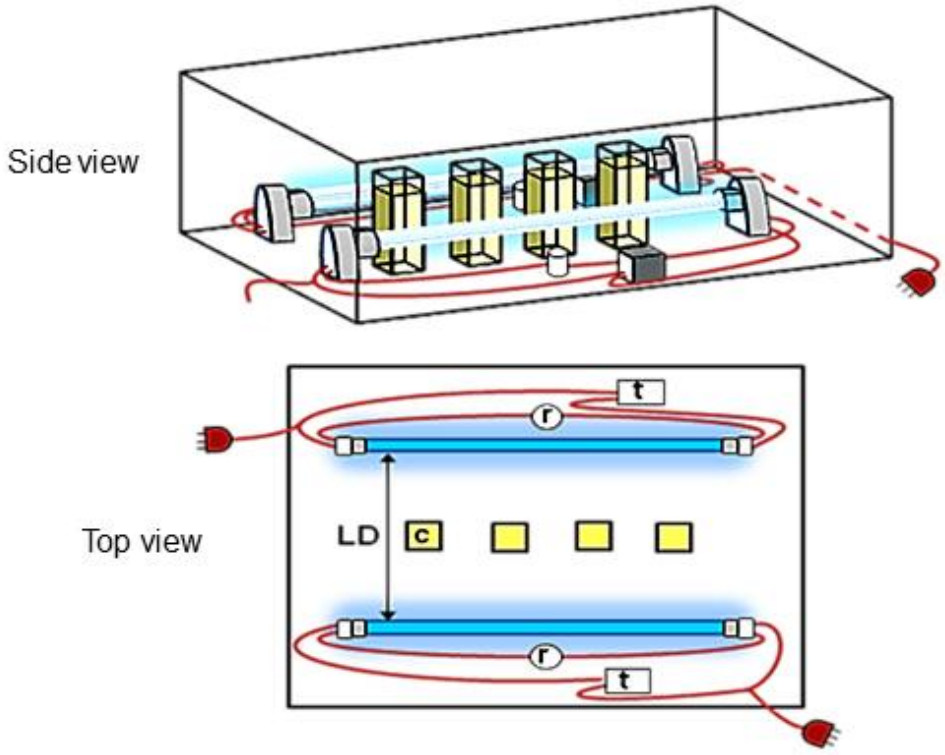

Fig. 2 Photoreactor. LD = distance between the lamps, C = quartz cells, r = reactance, t = transformer.

2.4. Optimization of the parameters affecting the fluorescence signal

A five-level central composite design of 17 experiments was applied for investigating the influence of the three variables on the fluorescence intensity, with three replicates at the central point. These variables were the concentration of hydrochloric acid (C_{HCl}), the irradiation time (IT) and the distance between the lamps (LD). The fluorescence intensity was recorded for each solution using 308 and 410 nm as excitation and emission wavelengths

145 respectively. The runs were carried out in a randomized sequence to minimize the effect of
146 uncontrolled variables on the response. The resulting experimental matrix is detailed in Table
147 1, and the quadratic regression model selected to define the relationship between the response
148 and the variables was:

149

$$F = b_0 + \sum_{i=1}^{3} b_i x_i + \sum_{i=1}^{3} b_{ii} x_i^2 + \sum_{i=1}^{3} \sum_{j=i+1}^{3} b_{ij} x_i x_j + e \quad (1)$$

150

151 where F is the response, x_i and x_j are the studied factors, b_0, b_i, b_{ii} and b_{ij} are the intercept,
152 linear, quadratic and interaction coefficients, and e the model error.

153

Table 1
Design generated for a central composite design and the obtained response values.

Run	b_1–C_{HCl}/M	b_2–IT/min	b_3–LD/cm	F (response)
1	1.50	1.00	6.00	5.8
2	1.50	30.00	6.00	24.7
3	2.50	7.00	8.00	16.7
4	3.00	16.00	6.00	32.6
5	2.50	25.00	3.50	25.4
6	0.30	16.00	6.00	14
7	1.50	16.00	10.00	26.5
8	1.50	16.00	6.00	31.8
9	0.50	7.00	8.00	15.4
10	0.50	25.00	3.50	6.4
11	0.50	25.00	8.00	21.8
12	1.50	16.00	6.00	33.6
13	2.50	25.00	8.00	29.2
14	1.50	16.00	2.00	23.6
15	1.50	16.00	6.00	33.7
16	2.50	7.00	3.50	24.7
17	0.50	7.00	3.50	6.3

C_{HCl}: concentration of hydrochloric acid; IT: irradiation time; LD: distance between the lamps.

154

155 *2.5. Quantitative analysis*

156

157 Preliminary experiments indicated that, under the established working conditions, linearity
158 is held until 61 ng mL^{-1}, which was the limiting assayed concentration in subsequent
159 analyses.

160 A calibration set of 9 samples was prepared, by duplicate, measuring appropriate aliquots
161 of stock solution of CBZ into 2.00 mL calibrated flasks, evaporating the solvent with nitrogen
162 and completing to the mark with 2 mol L^{-1} HCl. A validation set was similarly prepared
163 employing concentrations different from those used for calibration and following a random
164 design. With the purpose of evaluating the proposed strategy in the presence of these
165 interferent agents, twenty additional test samples containing random concentrations of CBZ
166 and these foreign compounds were prepared. The interferents were evaluated at the following
167 concentration ranges: 0–5600, 0–1200, 1–9, and 0–5000 ng mL^{-1} for ibuprofen, diclofenac,
168 piroxicam, and salicylic acid, respectively. The maximum level of each evaluated
169 interference was selected in order to avoid the saturation of the fluorescence signal. Taking
170 into account that the highest CBZ concentration was about 60 ng mL^{-1}, with the exception of
171 piroxicam, each interferent agent was between 16 and 90 times more concentrated than the
172 analyte.

173

174 *2.6. Real water samples*

175

176 All investigated water samples were prepared by spiking them with CBZ at three different
177 concentrations, obtaining levels between 0.4 and 5.5 ng mL^{-1}. Tap water from Rosario city
178 (Santa Fe, Argentina) and underground water from Funes and Venado Tuerto cities (Santa
179 Fe, Argentina) samples were used as received. The Paraná River sample was collected near

Rosario city, and after spiking it with CBZ, it was filtered through a filter paper to remove suspended solid materials. In order to improve the sensitivity of water analysis, a solid-phase extraction (SPE) procedure with C18 membranes was applied. Prior to sample application, each membrane was conditioned with 500 µL of methanol. Positive pressure was used to force the water sample through the membrane. For concentrations of CBZ at sub-part-per-billion levels, 50.0 mL of sample was employed, while a volume of 10.0 mL was used for the remaining samples. Following the extraction, the disk was dried by forcing air through it using a 25 mL syringe. Then, the retained CBZ was eluted with 500 µL of methanol and the liquid was collected in a 2.00 mL volumetric flask. After evaporation of the solvent with nitrogen, the residue was reconstituted to the mark with 2 mol L^{-1} HCl. Thus, the preconcentration factors were 25 and 5 for samples with sub-part-per-billion and part-per-billion concentrations, respectively. Then, the procedure described above was performed.

2.7. Software

The experimental design and optimization was carried out using Design Expert 6.0 (Stat-Ease, Inc.). The employed chemometric algorithms were written in MATLAB 7.6 [63]. PARAFAC, U- and N-PLS/RBL were implemented using the graphical interface of the MVC2 toolbox, which can be freely downloaded from the webpage www.iquir-conicet.gov.ar/descargas/mvc2.rar. MCR-ALS is available in the Internet at http://www.mcrals.info/. Theoretical considerations of the applied algorithms can be found in the supplementary information.

3. Results and discussion

205 *3.1. Preliminary studies*

206

207 As was previously indicated, CBZ does not display native fluorescence, but emission can
208 be obtained upon UV irradiation under certain working conditions, indicating the formation
209 of one or more emissive photoproducts (Fig. 3A). In the literature, different CBZ
210 photoproducts have been reported depending on the employed experimental conditions.

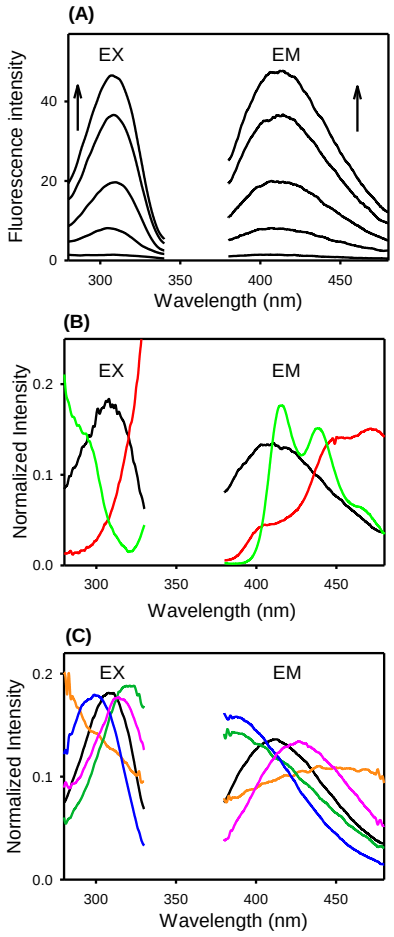

211

212 **Fig. 3** (A) Excitation and emission fluorescence spectra of CBZ photoproducts (initial C_{CBZ} =
213 0, 10.1, 25.3, 48.0, and 60.0 ng mL^{-1}). (B) Normalized excitation and emission fluorescence
214 spectra of CBZ photoproducts (black line), acridine (red line) and acridone (light green line).
215 (C) Normalized excitation and emission fluorescence spectra of CBZ (black line), ibuprofen
216 (orange line), diclofenac (green line), piroxicam (blue line), and salicylic acid (pink line) after
217 irradiation under the used experimental condition.
218

For example, acridine and acridone were the main identified photoproducts when an acid solution of CBZ was irradiated with a 1500 W arc xenon lamp during 30 min [64]. CBZ treatment with UV irradiation (17 W mercury lamp, 254 nm) in the presence of H_2O_2 produced acridine, a series of acridine intermediates and small amounts of salicylic acid, catechol and anthranilic acid among the reaction products [65]. Chiron et al. studied the photodegradation of CBZ in artificial estuarine water, mimicking natural processes [7]. After evaluating different experimental conditions, it was concluded that besides acridine (the major photodegradation intermediate), 10-hydroxycarbamazepine, hydroxyacridine-9-carboxaldehyde, and acridone are also formed.

Under our working conditions, the obtained wide spectra with excitation and emission maxima at 308 and 410 nm respectively, do not suggest a significant contribution of either acridine or acridone (Fig. 3B). However, regardless of the nature of the formed photoproducts, a linear relationship between the CBZ concentration and the obtained fluorescence intensity was corroborated and, therefore, a quantitative analysis could be properly developed.

3.2. Optimization of the experimental conditions

Exploratory experiments showed that the type and concentration of acid used in the reaction medium, the time of sample irradiation and the distance between the reactor lamps (the sample is positioned equidistant between both lamps) had critical effects on the photochemically induced fluorescence. Although in some systems the presence of different organized media could sensitize photochemical reactions [66,67], in our working conditions selected surfactants (sodium dodecyl sulfate, hexadecyltrimethylammonium bromide, Triton X-100) and cyclodextrins (β-, γ-, α- and 2-hydroxy-propil-β cyclodextrins) did not produce a

244 significant signal improvement. On the other hand, desoxigenation of the medium with a flow
245 of nitrogen did not improve the signal intensity.

246 As regards the acid employed, nitric, sulfuric and hydrochloric acids were checked. In the
247 presence of nitric acid, signals were not detected, and the sulfuric acid background signal was
248 significant. Hydrochloric acid produced the best signals and, therefore, it was selected for the
249 subsequent experiments.

250 It was found that irradiation with two 4 W lamps, rather than using either one 4 W lamp or
251 8 W lamps, produced an efficient photodegradation reaction of CBZ. Besides, the distance
252 between these lamps and the time of irradiation modified the signal. These factors were
253 optimized using a surface response methodology. Table 2 displays the ANOVA results for
254 the selected quadratic model, where it can be appreciated that the variables explain the data
255 and indicate that the variable effect is significant at 95 % confidence level. The coefficients
256 estimated for the mathematical model in terms of actual factors were: –40, 31, 2.3, 6.9, –5.2,
257 –0.08, –0.48, –1.5 for intercept, C_{HCl}, IT, LD, $(C_{HCl})^2$, $(IT)^2$, $(LD)^2$, C_{HCl}×LD and IT×LD,
258 respectively.

259 The optimum values obtained for C_{HCl}, IT and LD were 2 mol L^{-1}, 20 min and 6 cm,
260 respectively. These conditions were used for the corresponding quantitative analysis.

261 It is important to point out that the geometry of the photoreactor (Fig. 2) allows the
262 simultaneous irradiation of four solutions contained in the quartz cells. Thus, the time of
263 irradiation is equivalent to 5 minutes per sample.

264

265 *3.3. Quantitative analysis*

266

267 The purpose of the present work is to determine CBZ in natural matrices where other
268 concomitantly present compounds are potentially able to produce interference through either

269 themselves or their fluorescent photoproducts when the sample is subjected to the irradiation
270 protocol. Therefore, different pharmaceuticals selected from the list of organic
271

Table 2
Analysis of variance (ANOVA) for the selected quadratic model.[a]

Source	Sum of squares	DF	Mean square	F value	$p > F$
Model	1408.40	8	176.05	23.46	< 0.0001
b_1–C_{HCl}	511.89	1	511.89	68.22	< 0.0001
b_2–IT	151.89	1	151.89	20.24	0.020
b_3–LD	58.01	1	58.01	7.73	0.0239
b_{11}	179.14	1	179.14	23.87	0.0012
b_{22}	464.96	1	464.96	61.978	<0.0001
b_{33}	88.71	1	88.71	11.82	0.0088
b_{13}	97.37	1	97.37	12.98	0.0070
b_{23}	45.05	1	45.05	6.00	0.0399
Lack of Fit					0.100

[a] The term b_{12} was not significant ($p > 0.05$) and was excluded of the analysis. DF = degree of freedom; p = probability; R^2 (coefficient of determination) = 0.959; Pred R^2 (measures how well the model will predict the responses for a new experiment) = 0.794; Adeq precision (measures the signal to noise ratio) = 13.97.

272

273 micropollutants usually detected in the aquatic environment were checked as potential
274 interferents, namely ibuprofen, diclofenac, piroxicam, salicylic acid, naproxen, ketoprofen
275 and atenolol [11,68]. We found that, after irradiation, the excitation and emission spectra of
276 the photoproducts of the first four compounds (Fig. 1) are significantly overlapped with those
277 corresponding to CBZ ones, producing a severe interference (Fig. 3C). Thus, for improving
278 the selectivity of the method, a second-order calibration applying algorithms which achieve
279 the so-called second-order advantage was proposed.

280

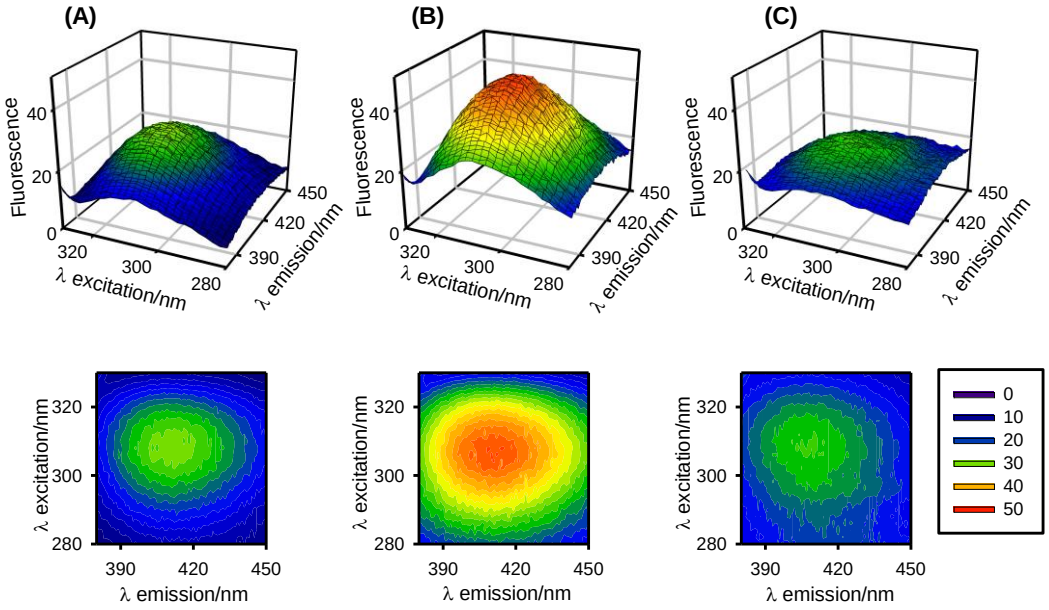

Fig. 4 Three-dimensional plots and the corresponding contour plots of excitation-emission photoinduced fluorescence matrices for (A) a validation sample containing 48.0 ng mL^{-1} CBZ, (B) a test sample containing 56.0 ng mL^{-1} CBZ, 2000 ng mL^{-1} ibuprofen, 1500 ng mL^{-1} salicylic acid, 600 ng mL^{-1} diclofenac and 2 ng mL^{-1} piroxicam, and (C) a spiked river sample after solid-phase extraction (original C_{CBZ} = 5.5 ng mL^{-1}).

Firstly, EEPIFMs of CBZ photoproducts under optimal working conditions were recorded for calibration and validation samples (Fig. 4A), where only the studied analyte is present. These matrices were successfully resolved by usual second-order algorithms such as PARAFAC, U-PLS, N-PLS and MCR-ALS (data not shown). However, the results were different when test samples containing interferent agents were processed. Fig. 4B shows the three-dimensional plot of the EEPIFM for a typical sample with interferences and the corresponding contour plot. The results obtained with different algorithms applied to these samples are discussed below.

3.3.1. PARAFAC

299 The PARAFAC model allowed us to obtain physically interpretable profiles. The
300 identification of the analyte was done with the aid of the estimated excitation and emission
301 profiles, and comparing them with those for an irradiated standard CBZ solution. The number
302 of components was selected by the so-called core consistency analysis [69], which consists in
303 studying the structural model based on the data and the estimated parameters of gradually
304 augmented models. A PARAFAC model is considered to be appropriate if incorporating an
305 additional component does not improve the fit considerably [69]. The number of components
306 also was analysed through the spectral profiles produced by the addition of a new component.
307 If this addition generated repeated profiles, suggesting overfitting, this new component was
308 discarded. The number of responsive components obtained using both procedures was two in
309 validation samples and three in samples with interferents. In validation samples, the obtained
310 number of components could be justified taking into account the presence of two different
311 signals corresponding to CBZ and background signals. On the other hand, in test samples
312 interferences are extracted as a single signal.
313 PARAFAC was initialized with the loadings giving the best fit after a small number of
314 trial runs, selected from the comparison of the results provided by generalized rank
315 annihilation and several random loadings [70].
316 Fig. 5A shows the prediction results corresponding to the application of PARAFAC to the
317 20 samples with interferents. As can be appreciated, the results are rather poor. This fact may
318 be explained considering the significant spectral overlapping among the analyte and
319 interferences, which precludes the successful decomposition of the second-order data [71].
320 The elliptical joint confidence region (EJCR, [72]) test for the slope and intercept of the
321 found vs. nominal concentrations plot shows that the ideal point (1,0) lies outside the EJCR
322 surface (Fig. 5F), also suggesting that PARAFAC is inappropriate for resolving the system
323 under investigation.

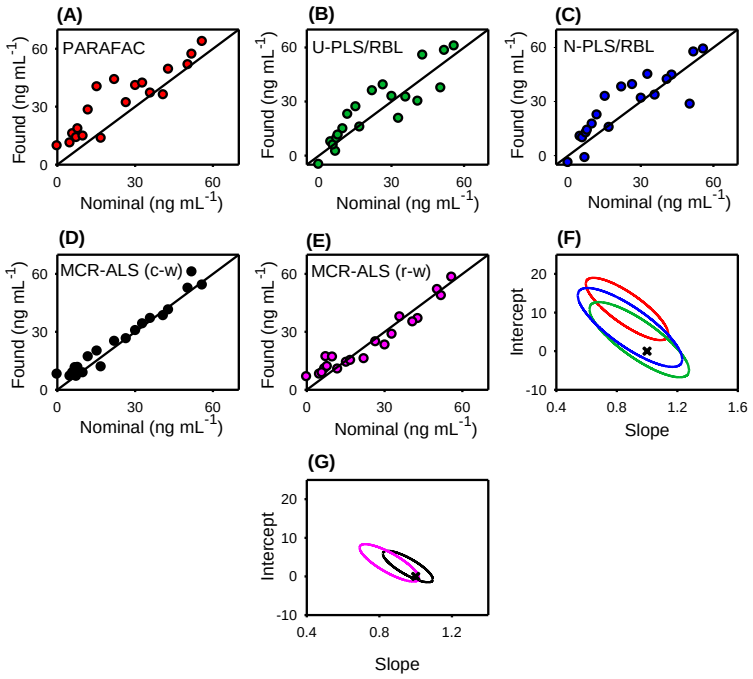

Fig. 5 Plots for CBZ predicted concentrations in samples with interferences (test samples) as a function of the nominal values using (A) PARAFAC, (B) U-PLS/RBL, (C) N-PLS/RBL, (D) MCR-ALS (column-wise augmentation), and (E) MCR-ALS (row-wise augmentation). Solid lines indicate the perfect fits. (F) Elliptical joint regions (at 95 % confidence level) for slope and intercept of the regression of PARAFAC (red line), U-PLS/RBL (green line), and N-PLS/RBL (blue line). (G) Elliptical joint regions (at 95 % confidence level) for slope and intercept of the regression of MCR-ALS using column-wise (black line) and row-wise (pink line) augmentations. Crosses in (F) and (G) mark the theoretical (intercept = 0, slope = 1) point.

3.3.2. U- and N-PLS

In the cases of U- and N-PLS/RBL, the optimum number of factors for the calibration set applying the cross-validation method described by Haaland and Thomas [73] was also two. When these algorithms were applied to samples containing interferents, in addition to the latent variables estimated from the calibration set, they required the introduction of the RBL procedure with an additional number of components corresponding to the unexpected sample constituents. This number, estimated by suitable consideration of RBL residues [74], ranged

344 from 1 to 2. Adding more unexpected components did not improve the fit. Apparently,
345 PLS/RBL considers the profiles of the four interferences as additional one or two
346 components, and is able to distinguish these combined signals from those of the analyte and
347 the blank. Figs. 5B and 5C show the prediction results corresponding to the application of U-
348 PLS/RBL and N-PLS/RBL to the samples containing interferences. In these figures, some
349 dispersion of the predictions with respect to the perfect fit lines is verified. While the
350 corresponding ellipses include the theoretical (1,0) point (Fig. 5F), they show large (and
351 undesirable) sizes. However, although these algorithms have some difficulty to solve the
352 system under study, they are more flexible and render better results than PARAFAC.
353
354 *3.3.3. MCR-ALS*
355
356 The MCR-ALS model decomposes an augmented data matrix, built by placing matrices
357 for different samples adjacent to each other, in such a way that the augmentation mode is the
358 one affected by the profile overlapping. As a result, the poor selectivity in the affected
359 dimension is recovered in the augmented dimension. In the present system, since a significant
360 overlapping between analyte and interferences is observed in the excitation and emission
361 spectra, both modes of augmentation were checked. Therefore, two different data processing
362 were performed: one of them comprised the building of augmented column-wise (emission
363 spectral) data matrices containing the test sample data and the calibration data matrices, and
364 the other one comprised the building of augmented row-wise (excitation spectral) data
365 matrices, also containing the test and calibration data matrices.
366 Before starting resolution, the determination of the number of MCR components was
367 estimated by applying singular value decomposition (SVD). Usually, the plot of singular
368 values as a function of principal component number is visually inspected, locating a number

for which the plot stabilizes. This number is initially employed for MCR-ALS analysis, and is afterwards refined (increased or decreased) until an appropriate solution is found, with a reasonable least-squares fit and physically recognizable profiles. Given the number of responsive components, their spectra were then obtained from the analysis of the so-called "purest" spectra, based on the SIMPLISMA methodology, a multivariate curve resolution algorithm which extracts the purest spectra of the mixture from a series of spectra of mixtures of varying composition [75]. The spectra provided by SIMPLISMA were suitable to perform the resolution and, therefore, it was not necessary to include reference spectra for the analyte as initial estimates for MCR-ALS. In the present system, the number of MCR components in both augmentation modes was three. Apparently, the algorithm combines the signals of interferents but perfectly distinguishes them from those belonging to the analyte and, as will be shown below, yields very good predictions.

During the iterative procedure leading to chemically recognizable solutions the constraint of non-negativity in both data modes was applied. The selected MCR convergence criterion was 0.1% (relative change in fit for successive iterations) and the maximum number of iterations was set to 1000. Convergence was achieved after less than 300 iterations in most of the evaluated samples. Further, the quality of the MCR-ALS recovered spectral profiles was evaluated using the criterion of similarity which involves a comparison, through the correlation coefficient (R) between the reference and evaluated spectrum [76]. The value of R found for CBZ photoproducts in the excitation and emission spectra were 0.9992 and 0.9997, respectively, corroborating the excellent quality of the MCR-ALS obtained results.

Figs. 5D and 5E show the prediction results corresponding to the application of MCR-ALS to the same test samples described above using the column and row-wise augmentation respectively. As can be observed, in both cases the predictions are in good agreement with the corresponding nominal values, with the results of column-wise augmentation being

394 slightly better. This fact could be ascribed to the better selectivity achieved through the
395 excitation spectra. The EJCR test (Fig. 5G) corroborates that both ellipses have a small size
396 and include the theoretically expected values of (1,0), demonstrating the accuracy of the used
397 methodologies.

398 The statistical results are complemented with the values shown in Table 3. The relative
399 error of prediction indicates acceptable precision, and both the limit of detection (LOD) and
400 limit of quantification (LOQ) obtained are suitable, taking into account that a very simple
401 methodology is applied to a complex multicomponent system.

Table 3
Statistical results for CBZ using the proposed methodolgy and MCR-ALS (column-wise augmentation).

	Test samples[a]	Real water samples[b]	Real water samples[c]
LOD[d] (ng mL^{-1})	5	1	0.2
LOQ[e] (ng mL^{-1})	15	3	0.6
RMSEP[f] (ng mL^{-1})	4	0.4	0.1
REP[g] (%)	13	7	2

[a] Twenty samples containing ibuprofen, diclofenac, piroxicam, salicylic acid as interferents.
[b] Preconcentration factor = 5 (the results refer to the original water sample before SPE).
[c] Preconcentration factor = 25 (the results refer to the original water sample before SPE).
[d] LOD, limit of detection calculated according to ref. 78.
[e] LOQ, limit of quantitation calculated as LOD×(10/3.3).
[f] RMSEP, root-mean-square error of prediction.
[g] REP, relative error of prediction.

402

403

404 The latter two figures of merit have been estimated using the expressions recommended by
405 IUPAC for the detection capabilities, which take into account the so-called Type 1 and 2
406 errors (false detects and false non-detects respectively) [77]. They were applied to the
407 pseudo-univariate calibration plot (analyte scores vs. nominal concentrations) provided by
408 MCR-ALS, as previously suggested [78].

409

410 *3.4. Real water samples*

411

412 With the purpose of evaluating the present method in real samples and demonstrating its
413 ability of overcoming the interference from background matrices, waters from different
414 origins were analysed. CBZ is detected in water bodies in a wide range of concentrations,
415 generally in the order of part- and sub-part-per-billion levels. Therefore, the sensitivity of the
416 present method was improved using a pre-concentration step by employing C18 membrane-
417 SPE. At this point, it is necessary to point out that the selection of C18 membranes is based
418 on our excellent experience with this solid-support as extractor of organic compounds
419 [79−81]. Although other materials could be used for the extraction procedure, previously
420 reported experiments performed with different commercial and in-house ion-exchange
421 polymeric sorbents were not successful for CBZ extraction [82].

422 Fig. 6A shows both the excitation and emission spectra of CBZ photoproducts and the
423 signal of a typical real water sample after the SPE procedure. As can be seen, the selected
424 sample (river water) shows intense fluorescence signals in the same region where the CBZ
425 photoproducts emit, which are ascribed to dissolved organic matter [83]. These overlapping
426 would preclude the direct measurement of the analyte, but it does not represent a problem
427 when using second-order approaches. Fig. 4C shows both three-dimensional plot of the
428 EEPIFM and the corresponding contour plot of real sample of river spiked with CBZ and
429 treated with C18 membrane.

430 A recovery study was performed by spiking water samples with appropriate amounts of
431 CBZ, in triplicate, at three different concentration levels, following the treatment indicated in
432 the experimental section. According to the previous results, MCR-ALS was selected to
433 resolve these samples, and the outstanding results obtained (Table 4, Fig. 6B) suggest that the
434 method can overcome the problem of the presence of unexpected interferents from the

435 background of the real samples. Table 3 displays the corresponding figures of merit obtained
436 for these samples.

437 In comparison with the performances of selected methods for the determination of CBZ in
438 natural waters (Table 5), limits of detection from 0.2×10^{-3} to 10 ng mL^{-1} have been found
439 using different strategies, all using pre-concentrations procedures and most of them applying
440 chromatographic (separation) approaches. In the present case, a low limit of detection is
441 achieved in real samples (LOD = 0.2 ng mL^{-1}) applying a non-sophisticated method and
442 without using organic solvents. Note a solid-phase extraction procedure using a higher
443 amount of sample (> 50 mL) allows decrease even more the LOD. Additionally, a sampling
444 rate of about six samples per hour (including the EEPIFM measuring) makes the method very
445 advantageous.

446

Table 4
Recovery study of CBZ for spiked water samples.[a]

Sample	Taken (ng mL^{-1})	Found (ng mL^{-1})[b]	Recovery (%)
Underground water	0.70	0.8 (0.2)	114
(Funes City)	2.00	2.3 (0.3)	115
	4.00	4.5 (0.9)	112
Underground water	0.40	0.47 (0.01)	117
(Venado Tuerto City)	3.00	2.8 (0.1)	93
	5.00	5.5 (0.2)	110
Tap water	0.80	0.86 (0.02)	107
(Rosario City)	1.20	0.93 (0.01)	78
	4.50	4.0 (0.2)	89
River water	0.00	ND[c]	
(Paraná River)	2.50	2.7 (0.5)	108
	5.50	6.1 (0.1)	111

[a] using MCR-ALS algorithm (column-wise augmentation).
[b] Mean of three determinations. Standard deviations between parentheses.
[c] ND, not detected.

447

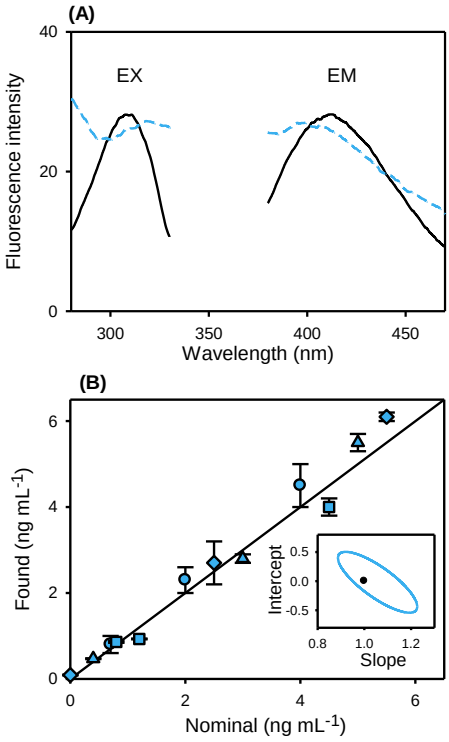

Fig. 6 (A) Excitation and emission fluorescence spectra of CBZ photoproducts (C_{CBZ} = 40.0 ng mL^{-1}, black line) and background signals of a river sample without CBZ after the SPE treatment (sky-blue dashed line). (B) Plot for MCR-ALS predicted concentrations of CBZ as a function of the nominal values in a river (diamonds) and tap water (squares) samples, and in two different underground water samples (circles and triangles) spiked analyte (error bars correspond to triplicates). The inset shows the corresponding elliptical joint region at 95% confidence level. The cross marks the theoretical (intercept = 0, slope = 1) point.

4. Conclusions

A novel and simple fluorimetric method for carbamazepine (CBZ) determination was developed and successfully applied to the quantitation of this emerging contaminant in water samples. Analyses were accomplished in a significant short time, with a minimum operator effort and avoiding the use of organic solvents. The selectivity of the method is achieved through the coupling of multivariate calibration. Among the different second-order algorithms investigated, multivariate curve resolution-alternating least-squares (MCR-ALS) showed a superior predictive capability and would be the recommended one in situations where interferences present similar profiles as the investigated compound.

Table 5
Analytical performance of selected methods reported for the determination of CBZ in natural waters.

Method	VS[a]	Concentration level[b]	RSD[c] and REC[c]	Sample	Ref
SPME-GC-MS	4	LOD = 1.0	RSD = 12.0	GW, SW	[20]
SPE-GC-MS	1000	LOD = 6.5×10^{-3} (nanopure water). LOD = 8.7×10^{-3} (SW); 0.035–0.060 (lake); 0.030–0.250 (river); 0.100–0.800 (WWTP)	REC = 46-65 (0.100 ng mL^{-1})	SW, STPEs	[21]
SPE-GC-MS	1000	LOD = 9.6×10^{-3}; LODet = 32×10^{-3}	REC = 80 (TW) and 74 (SW)	TW, SW	[22]
SPE-HPLC-PIF	250	Without SPE: LOD = 30; LOQ = 100. With SPE: 12 (SS with 10 ng mL^{-1} added)	RSD = 3.4	STP-WW	[23]
SPE-LC-MS/MS		STPI: 0.369. STPE: 0.426. SW (river): 0.7×10^{-3}. SS: 0.100	REC = 83.6 -103.5; RSD = 5.9	STPI, STPE, SW	[24]
SPE-GC-MS and SPE-LC-MS/MS	500-1000	MC = 1.2	Absolute REC = 89 (GC) and 99 (LC)	STPEs	[25]
SPE-GC-MS	500	LOD = 2.2; LOQ = 0.074	REC = 67	Municipal STP	[26]
SPE-LC-MS/MS		STPI: 0.356; STPE: 0.251		STPI, STPE, biosolids	[27]
SPE-GC-MS (on-line derivatization)	50-500	LOQ = 8.0×10^{-3}	REC = 79-108	TW, SW, WWE, GW	[28]
SPE-HPLC-MS	500	LOQ = 1.3×10^{-3} (STPE); Found (STPE) = 0.033– 1.3	RSD = 0.7 % (10 ng/injected); RSD = 2.88 (100 ng /injected)	Urban WWs	[29]
SPE-HPLC-DAD	500-1000	WWI: LOD = 0.04; LOQ = 0.12. WWE: LOD = 0.02; LOQ = 0.06	REC = 95, RSD = 4.3	WWI, WWE	[30]
SPE-GC-MS	500	LOQ = 0.030	REC = 110; RSD = 11.5	River water	[31]
SPE-LC-MS/MS	100	LOD = 7; LOQ = 19	REC = 88.1 (1 ng mL^{-1}); RSD = 2.2	Hospital WWE	[32]
SPE-LC-MS/MS	100-1000	STPI: LOQ = 0.02; MC = 2. STPE: LOQ = 0.01; MC = 1.9. SW: LOQ = 0.002; MC = 0.081	Absolute REC = 36-98	STPI, STPE, SW, GW, DW	[36]
SPE (MIP)-LC-MS	100	1	REC = 80	WW	[38]
SPE-voltammetry		LOD = 9.4; LOQ = 33. SS: 500	REC = 95.8; RSD = 5.7	WW	[43]
Off- and on-line SPE-LC-QqQ-MS	500	LOD = 0.2×10^{-3}	RSD < 15	SW and DW	[15]
SPE-LDTD-APCI-MS/MS	100	0.012	RSD = 8	municipal WW	[45]
SPE-EEPIF	10-50	LOD = 1 (PCF = 5); LOD = 0.2 (PCF = 25)	REC = 78-117; REP = 2-7	SW, UW	This work

[a] VS, volume of sample in mL.
[b] For comparison, concentration units were unified to ng mL^{-1}.
[c] Relative standard deviation (RSD) and recovery (REC), both in %.
Abbreviations: APCI, atmospheric pressure chemical ionization; DW, drinking water; EEPIF, excitation-emission photoinduced fluorimetry; GW, groundwater; LC, liquid chromatography; LDTD, laser diode thermal desorption; LOD, limit of detection, LODet, limit of determination, LOQ, limit of quantification; MC, maximum found concentration; MIP, molecularly imprinted polymer; MS, mass spectrometry; MS/MS, tandem mass spectrometry; PCF, preconcentration factor; PIF, photoinduced fluorescence; QqQ, triple quadrupole; REP, relative error of prediction; REC, recovery; RSD, relative standard deviation; SPE, solid-phase extraction; SPME, solid-phase microextraction; SS, spiked sample; STP, sewage treatment plant; STPE, sewage treatment plant effluent; STPI, sewage treatment plant influent; SW, surface water; TW, tap water; UW, underground water; VS, volume of sample; WW, wastewater; WWE, wastewater effluent; WWI, wastewater influent.

466 **Acknowledgements**

467

468 The authors gratefully acknowledge Universidad Nacional de Rosario and Consejo Nacional
469 de Investigaciones Científicas y Técnicas (Project PIP 1950) for financially supporting this
470 work.

471

472 **References**

[1] A. Goodman Gilman, J.G. Hardman, L.E. Limbrid, Goodman & Gilman's the Pharmacological Basis of Therapeutics, 10th ed., Mc-Graw Hill, New York, 2001.

[2] S.D. Richardson, T.A. Ternes, Anal. Chem. 83 (2011) 4614.

[3] M. Schriks, M.B. Heringa, M.M.E. van der Kooi, P. de Voogt, A. van Wezel, Water Res. 44 (2010) 461.

[4] V.L. Cunningham, C. Perino, V.J. D'Aco, A. Hartmann, R. Bechter. Regul. Toxicol. Pharm. 56 (2010) 343.

[5] S. Madden, J.L. Maggs, B.K. Park, Drug Metab. Dispos. 24 (1996) 469.

[6] R. Andreozzi, R. Marotta, G. Pinto, A. Pollio. Water Res. 36 (2002) 2869.

[7] S. Chiron, C. Minero, D. Vione, Environ. Sc. Technol. 40 (2006) 5977.

[8] T. Kosjek, H.R. Andersen, B. Kompare, A. Ledin, E. Heath, Environ. Sc. Techn. 43 (2009) 6256.

[9] M. Gros, M. Petrović, D. Barceló, Anal. Bioanal. Chem. 386 (2006) 941.

[10] M. Petrović, D. Barceló, Trends Anal. Chem. 26 (2007) 486.

[11] C. Tixier, H.P. Singer, S. Oellers, S.R. Müller, Environ. Sc. Technol. 37 (2003) 1061.

[12] R. Loos, B.M. Gawlik, G. Locoro, E. Rimaviciute, S. Contini, G. Bidoglio, Environ. Pollut. 157 (2009) 561.

[13] R. Loos, G. Locoro, S. Comero, S. Contini, D. Schwesig, F. Werres, P. Balsaa, O. Gans, S. Weiss, L. Blaha, M. Bolchi, B. M. Gawlik, Water Res. 44 (2010) 4115.

[14] M. Clara, B. Strenn, N. Kreuzinger, Water Res. 38 (2004) 947.

[15] P.A. Segura, S.L. MacLeod, P. Lemoine, S. Sauvé, C. Gagnon, Chemosphere 84 (2011) 1085.

[16] J. Wang, P.R. Gardinali, Anal. Bioanal. Chem. 404 (2012) 2711.

[17] M. Furlanut, M.G. Delucca, G. Dilberis, A. Barnaba, Br. J. Clin. Pharmacol. 11 (1981) 393.

[18] J.L. Maggs, M. Pirmohamed, N.R. Kitteringham, B.K. Park. Drug Metab. Dispos. 25 (1997) 275.

[19] G.F. van Rooyen, D. Badenhorst, K.J. Swart, H.K.L. Hundt, T. Scanes, A.F. Hundt, J. Chromatogr. B 769 (2002) 1.

[20] M. Moeder, S. Schrader, M. Winkler, P. Popp, J. Chromatogr. A 873 (2000) 95.

[21] S. Öllers, H. Singer, P. Fässler, J. Chromatogr. A 911 (2001) 225.

[22] F. Sacher, F. Lange, H. Brauch, I. Blankenhorn, J. Chromatogr. A 938 (2001) 199.

[23] C. González Barreiro, M. Lores, M.C. Casais, R. Cela, J. Chromatogr. A 993 (2003) 29.

[24] X.S. Miao, C.D. Metcalfe, Anal. Chem. 75 (2003) 3731.

[25] R. Andreozzi, M. Raffaele, P. Nicklas, Chemosphere 50 (2003) 1319.

[26] M. Carballa, F. Omil, J.M. Lema, M. Llompart, C. García Jares, I. Rodríguez, M. Gómez, T. Ternes, Water Res. 38 (2004) 2918.

[27] X.S. Miao, J.J. Yang, C.D. Metcalfe, Environ. Sci. Technol. 39 (2005) 7469.

[28] W.C. Lin, H.C. Chen, W.H. Ding, J. Chromatogr. A 1065 (2005) 279.

[29] S. Castiglioni, R. Bagnati, D. Calamari, R. Fanelli, E. Zuccato, J. Chromatogr. A 1092 (2005) 206.

[30] J.L. Santos, I. Aparicio, E. Alonso, M. Callejón, Anal. Chim. Acta 550 (2005) 116.

[31] Z. Moldovan, Chemosphere 64 (2006) 1808.

[32] M.J. Gómez, M. Petrović, A.R. Fernández Alba, D. Barceló, J. Chromatogr. A 1114 (2006) 224.

[33] M.R. Hadjmohammadi, P. Ebrahimi, Anal. Chim. Acta 516 (2004) 141.

[34] H. Breton, M. Cociglio, F. Bressolle, H. Peyriere, J.P. Blayac, D. Hillaire Buys, J. Chromatogr. B 828 (2005) 80.

[35] T. Yoshida, K. Imai, S. Motohashi, S. Hamano, M. Sato, J. Pharm. Biomed. Anal. 41 (2006) 1386.

[36] D. Hummel, D. Löffler, G. Fink, T.A. Ternes, Environ. Sci. Technol. 40 (2006) 7321.

[37] D. Fatta, A. Nikolaou, A. Achilleos, S. Meriç, Trends Anal. Chem. 26 (2007) 515.

[38] A. Beltran, E. Caro, R.M. Marcé, P.A.G. Cormack, D.C. Sherrington, F. Borrull, Anal. Chim. Acta 597 (2007) 6.

[39] S. Wu, W. Xu, Q. Subhani, B. Yang, D. Chen, Y. Zhu, L. Li, Talanta 101 (2012) 541.

[40] Z. Rezaei, B. Hemmateenejad, S. Khabnadideh, M. Gorgin, Talanta 65 (2005) 21.

[41] B. Hemmateenejad, Z. Rezaei, S. Khabnadideh, M. Saffari, Spectrochim. Acta A 68 (2007) 718.

[42] M.S. Cámara, C. Mastandrea, H.C. Goicoechea, J. Biochem. Biophys. Methods 64 (2005) 153.

[43] A. Veiga, A. Dordio, A.J. Palace Carvalho, D. Martins Teixeira, J. Ginja Teixeira, Anal. Chim. Acta 674 (2010) 182.

[44] B. Unnikrishnan, V. Mani, S.M. Chen, Sensor Actuat B 173 (2012) 274.

[45] D.P. Mohapatra, S.K. Brar, R.D. Tyagi, P. Picard, R.Y. Surampalli, Talanta 99 (2012) 247.

[46] L. Vera Candioti, M.J. Culzoni, A.C. Olivieri, H.C. Goicoechea, Electrophoresis 29 (2008) 4527.

[47] Y.Y. Lin, C.C. Wang, Y.H. Ho, C.S. Chen, S.M. Wu, Anal. Bioanal. Chem. 405 (2013) 259.

[48] G.M. Escandar, D. González Gómez, A. Espinosa Mansilla, A. Muñoz de la Peña, H.C. Goicoechea, Anal. Chim. Acta 506 (2004) 161.

[49] S. Kuhn, N. Meier, O. Pierart, G. Godoy, Farmaco Ed. Prat. 37 (1982) 296.

[50] L. De la Peña, A. Gomez Hens, D. Pérez Bendito, Fresen. J. Anal. Chem. 338 (1990) 821.

[51] Z.T. Pan, L.F. Yao, Chin. J. Anal. Chem. 26 (1998) 997.

[52] Z.Q. Zhang, G.X. Liang, J. Ma, Anal. Lett. 39 (2006) 2417.

[53] C. Huang, Q. He, H. Chen, J. Pharm. Biomed. Anal. 30 (2002) 59.

[54] P. Anastas, N. Eghbali, Chem. Soc. Rev. 39 (2010) 301.

[55] J.A. Linthorst, Found Chem. 12 (2010) 55.

[56] R. Bro, Chemom. Intell. Lab. Syst. 38 (1997) 149.

[57] J. Öhman, P. Geladi, S. Wold, J. Chemom. 4 (1990) 135.

[58] A.C. Olivieri, J. Chemom. 19 (2005) 253.

[59] R. Bro, J. Chemom. 10 (1996) 47.

[60] R. Tauler, Chemometr. Intell. Lab. Syst. 30 (1995) 133.

[61] K.S. Booksh, B.R. Kowalski, Anal. Chem. 66 (1994) 782A.

[62] A. Rinnan, J. Riu, R.J. Bro, J. Chemom. 21 (2007) 76.

[63] MATLAB R2011b, The MathWorks Inc., Natick, MA, USA.

[64] V. Calisto, M.R.M. Domingues, G.L. Erny, V.I. Esteves, Water Res. 45 (2011) 1095.

[65] D. Vogna, R. Marotta, R. Andreozzi, A. Napolitano, M. d'Ischia, Chemosphere 54 (2004) 497.

[66] A.M. García Campaña, J.J. Aaron, J.M. Bosque Sendra, Talanta 55 (2001) 531.

[67] E.M. Almansa Lopez, A.M. García Campaña, J.J. Aaron, L. Cuadros Rodríguez, Talanta 60 (2003) 355.

[68] M. Stuart, D. Lapworth, E. Crane, A. Hart, Sci. Total Environ. 416 (2012) 1.

[69] R. Bro, H.L. Kiers, J. Chemom. 17 (2003) 274.

[70] P.C. Damiani, I. Durán Merás, A. García Reiriz, A. Jiménez Jirón, A. Muñoz de la Peña, A.C. Olivieri, Anal. Chem. 79 (2007) 6949.

[71] A.C. Olivieri, G.M. Escandar, A. Muñoz de la Peña, Trends Anal. Chem. 30 (2011) 607.

[72] A.G. González, M.A. Herrador, A.G. Asuero, Talanta 48 (1999) 729.

[73] D.M. Haaland, E.V. Thomas, Anal. Chem. 60 (1988) 1193.

[74] S.A. Bortolato, J.A. Arancibia, G.M. Escandar, Anal. Chem. 80 (2008) 8276.

[75] W. Windig, J. Guilment, Anal. Chem. 63 (1991) 1425.

[76] J. Kuligowski, G. Quintas, R. Tauler, B. Lendl, M. de la Guardia, Anal. Chem. 83 (2011) 4855.

[77] L. A. Currie, Anal. Chim. Acta 391 (1999) 127.

[78] J. Saurina, C. Leal, R. Compañó, M. Granados, M.D. Prat, R. Tauler, Anal. Chim. Acta 432 (2001) 241.

[79] G.N. Piccirilli, G.M. Escandar, F. Cañada Cañada, I. Durán Merás, A. Muñoz de la Peña, Talanta 77 (2008) 852.

[80] S.A. Bortolato, J.A. Arancibia, G.M. Escandar, Anal. Chem. 81 (2009) 8074.

[81] M. Bravo, L.F. Aguilar, W. Quiroz, A.C. Olivieri, G.M. Escandar, Microchem. J. 106 (2013) 95.

[82] D. Bratkowska, R.M. Marcé, P.A.G. Cormack, D.C. Sherrington, F. Borrull, N. Fontanals, J. Chromatogr. A 1217 (2010) 1575.

[83] N. Hudson, A. Baker, D. Reynolds, River Res. Appl. 23 (2007) 631.

Glossary

CBZ: carbamazepine.

C_{CBZ}*:* concentration of carbamazepine.

C_{HCl}*:* concentration of hydrochloric acid.

EEPIFMs: excitation-emission photoinduced fluorescence matrices.

EJCR: elliptical joint confidence region.

EU: European Union.

IT: irradiation time.

LD: distance between the lamps.

LOD: limit of detection.

LOQ: limit of quantification.

MCR-ALS: multivariate curve resolution-alternating least squares.

N-PLS/RBL: multidimensional partial least-squares/ residual bilinearization.

PARAFAC: parallel factor analysis.

PMT: photomultiplier tube.

R: correlation coefficient.

SPE: solid-phase extraction.

SVD: singular value decomposition.

U-PLS/RBL: unfolded partial least-squares/residual bilinearization.